FATIGUE CRACK INITIATION AND PROPAGATION IN A V/Nb DUAL-PHASE STEEL

K.Gerić* and Dj.Drobnjak**

The fatigue crack initiation and propagation behavior of a V/Nb dual-phase steel has been studied. The parameter $\Delta K/\sqrt{\rho}$ was used to normalize data concerning crack initiation at three notch tip radii (0.4, 0.8 and 1.6 mm). The value of $(\Delta K/\sqrt{\rho})_{th}$ was found to decrease from 830 to 720 and 630 MPa with increasing notch tip radius from 0.4 to 0.8 and 1.6 mm respectively, and is not to be taken as a threshold independent on the crack tip geometry. The fatigue crack propagation threshold is estimated at 14,7 MPa$\sqrt{m}$. The fatigue crack growth rate as a function of stress intensity range can be described by the following relation: $da/dN=2.7\cdot10^{-11}(\Delta K)^{2.22}$. Scanning electron microscopy was used to study the effect of martensite, which coexist with ferrite in dual-phase steels, on fatigue crack propagation.

INTRODUCTION

Microstructure, tensile and strain-hardening properties of dual-phase steels have been studied in many details. For instance, a number of international conferences have been devoted to dual-phase steels |1-3|. However, fatigue properties, and in particular the fatigue crack initiation and propagation thresholds, $(\Delta K/\sqrt{\rho})_{th}$ and ΔK_{th} respectively,as well as the fatigue crack growth rate, da/dN, and their relation to microstructure have been less extensively studied. Some results, which are concerned with the effect of prior deformation on fatigue life (Sherman and Davies |4|), the effect of dual-phase structure on crack initiation (Kim and Fine |5|) and crack propagation (Suzuki and McEvily |6|),(Minakawa et al. |7|) are far from comprenhensive.

The aim of this work was to determine the crack initiation and propagation thresholds as well as the crack growth rate as a function of the stress intensity range in a typical dual-phase steel, and to study the role of martensite in the crack propagation process in the near threshold region in which microstructure influence is known to be of importance.

EXPERIMENTAL PROCEDURE

Material. The material used in this study had a composi-

* Faculty of Mechanical Eng.,N.Sad,Yugoslavia

** Faculty of Technology and Metallurgy,Belgrade,Yugoslavia

tion (in wt. pct) of 0.083 C, 1.44 Mn, 0.33 Si, 0.039 Al, 0.045 Nb and 0.072 V. Specimens, 7.5 mm thick, 20 mm wide and 60 mm long were machined from the as-received 8 mm thick hot rolled sheet, and subsequently subjected to a heat treatment which consisted of intercritical annealing at 800 ^{o}C for 15 min. followed by step quenching first into an oil bath at 250 ^{o}C and then, after 10 min. into water. This heat treatment is shown to produce a dual phase structure, with the following tensile properties: yield strenght 338 MPa, tensile strength 655 MPa and elongation 24% (Radmilovic V. et al. |8,9|).

Fatigue Specimen. A modified three point bend test configuration, similar to a modified compact tension configuration (Braglia et al. |10|), was used for crack initiation and propagation studies (Fig.1). The normal V notch was replaced by a finite radius notch (ρ=0.4, 0.8 and 1.6 mm). Notches were placed such that loading would always be parallel to the rolling direction. Notches were introduced using an abrasive wire saw. After machining a notch the fatigue specimens were polished and then a set of parallel lines traced first at 0.25 mm from the notch tip and then at 0.5 mm intervals on the polished surface.

Fatigue Testing. The fatigue tests were carried out on a 20 kN Amsler testing machine. All tests were run under load control at a frequency of 80 Hz, with Fmin/Fmax=0.2.

Crack initiation and subsequent crack propagation were observed continously with a travelling microscope at a magnification of 30 times. The number of cycles was recorded (with an accuracy of ±500 cycles), first after a 0.25 mm long crack was developed and then each time the crack lenght was increased for additional 0.5 mm. Crack initiation life was defined as the development of a 0.25 mm long crack |10|. This definition includes both the actual crack initiation and subsequent propagation to a length of 0.25 mm. In the present study only a relatively low ΔK range, which needed more then $5 \cdot 10^4$ cycles to develope a 0.25 mm long crack, was used thus ensuring a minimum accuracy in recording the number of cycles of about ±1%.

The stress intensity was calculated using an equation given for the three point bend test specimen |11|, while the crack growth rate was found by using the incremental polynomial method |12|.

In the determination of the threshold stress intensity range, ΔK_{th}, a stepwise ΔK-decreasing test was used |6,7|. The crack was initially grown 1 mm from the notch tip, and the load was then shed in 10 pct decrements. The crack was each time allowed to grow 0.5 mm. This procedure was followed until a stress intensity range was reached at which no growth was detected in 10^6 cycles. This stress intensity range was defined as the threshold level, ΔK_{th}.

SEM and Metallographic Investigation. Scanning electron microscopy (SEM) was used to study the fracture surface, while the propagation path was studied by both SEM and metallographic technique using an etching reagent consisting of 1% water solution of sodium metabisulfite and 4% ethylalchol solution of picric acid in 1:1 volume ratio (Le Pera |13|).

RESULTS

Fatigue Crack Initiation. Results concerning crack initiation at three notch radii are presented in Figs.2 and 3. Plots of crack initiation life, N_i, versus stress intensity range, ΔK, and versus $\Delta K/\sqrt{\rho}$ parameter are shown in Figs. 2 and 3 respectively. The results show that the number of cycles needed for crack initiation increases with decreasing stress intensity range (Fig. 2) and the parameter $\Delta K/\sqrt{\rho}$ (Fig.3). In this regard it is important to note that a distinct separation of the results for each notch radius is observed for both ΔK vs. N_i and $\Delta K/\sqrt{\rho}$ vs. N_i plots in the entire range tested ($5 \cdot 10^4$ to 10^6 cycles). The results of Fig. 3 show that at 10^6 cycles the $\Delta K/\sqrt{\rho}$ parameter decreases from 830 to 720 and 630 MPa with increasing notch tip radius from 0.4 to 0.8 and 1.6 mm respectively.

Fatigue Crack Propagation. Fatigue crack propagation threshold ΔK_{th} is estimated at about 14.7 MPa$\sqrt{m}$. Fatigue crack growth rate, da/dN, as a function of stress intensity range, ΔK, for 6 specimens is shown in Fig. 4. While a considerable scatter is encountered in crack growth rate experiment, a relation of the form.

$$da/dN = 2.7 \cdot 10^{-11} (\Delta K)^{2.22} \qquad (1)$$

is found to represent the experimental data reasonable well. (The units are given in m/cicle and MPa$\sqrt{m}$.)

SEM results show a transgranular mode of fracture close to the notch tip (Fig.5), while a mixed mode of fracture is observed at a higher stress intensity range (Fig. 6). Among the other features the mixed mode is characterized by small facets in some areas (Fig. 6), intergranular and secondary cracks as well as fatigue striations in the others (Fig. 7). However, the metallographic investigation of the crack path in the near threshold intensity range shows that in addition to crack propagation in ferrite and along the ferrite/martensite interface, crack propagation through martensite is taking place (Fig. 8).

DISCUSSION

Fatigue Crack Initiation. The parameter $\Delta K/\sqrt{\rho}$ is previously found to normalize all initiation data from notches with different radii for longer initiation lives (Barsom et al |14|). However, the present results indicate (Fig. 3) that $\Delta K/\sqrt{\rho}$ parameter does not normalize experimental data even at 10^6 cycles. A trend exists where in a lower value of $\Delta K/\sqrt{\rho}$ is needed to initiate a crack as ρ increases. For each notch tip radius used in this study there seems to be a different threshold level, $(\Delta K/\sqrt{\rho})_{th}$. Samples cycled at or below this level would not be expected to initiate a crack in 10^6 cycles. This behaviour may be atrributed to a volume effect, which was previously seen at shorter initiation lives |10,14|. In this connection it is assumed that when a notch radius is increased, a greater volume of material is subjected to high stress at the notch root,what in turn increases the probability of creating a crack nucleation site (|14|, Rolfe and Barsom |15|).

According to Smith and Miller |16| the minimum stress required to initiate a fatigue crack is inversly proportional to fatigue crack concentration factor given by $(1+7.69\sqrt{D/\rho})^{0.5}$, where D and ρ are the notch depth and the root radius respectively. A decrease in ρ from 1.6 to 0.4 mm, as in the present case, bring an increase in Smith and Miller's concentration factor of about 26%, what is in good agreement with experimental data which shows that the stress required to initiate a crack at 10^6 cycles decreases for about 27%.

Fatigue crack initiation thresholds are usually related to tensile properties. There seems to be general agreement that threshold level decreases as yield strength increases (|5|,|15|, Fine |17|).However, published data for various types of steels (|5|,|10|,|15|) are not always consistent with this prediciton. For instance, while the Rolf and Barsom's empirical relation, $(\Delta K/\sqrt{\rho})_{th}=9.5(YS)^{2/3}$ (where the units are given in MPa$\sqrt{m}$ and MPa), holds for a number of ferrite-pearlite and martensitic steels having yield strength (YS) in the range from about 276 to 965 MPa |15|, it seems to break down for some HSLA steels, having YS in the range from 428 to 608 MPa |5|. This is particularly truth for the present as well as a previously tested GM 980X dual-phase steel |5|, which in spite of relatively low yield strength level; (338 and 448 MPa respectively)(accompanied by a low YS/UTS ratio 0.52 and 0.67 respectively, and a high strain hardening exponent; n=0.21) show a high resistance to fatigue crack initiation (Both steels show virtually equal threshold value of about 830-840 MPa if comparison is made at a similar notch tip radius, and using a similar criterion for defining the crack initiation life). This potentially makes dual-phase steels atractive not only because of their superior stretch formability but also because of their high resistance to fatigue crack initiation at a given yield strength level.

Fatigue Crack Propagation. In contrast to fatigue crack initiation threshold, the fatigue crack propagation threshold decrease as yield strength increase (|7|,|17|,Ritchie |18|). Thus threshold levels of quenched and tempered steels (YS≈500-1300 MPa) are generally lower (ΔK_{th}≈5-9 MPa$\sqrt{m}$) than those of normalized, normalized and tempered and annealed steels (YS≈300-400 MPa; ΔK_{th}≈7-10.5 MPa$\sqrt{m}$)(|7|,Ritchie |19|,Cooke |20|,Masounave and Bailon |21|). However, the fatigue crack propagation threshold of 14.7 MPa$\sqrt{m}$ determined in this work for a V/Nb dual phase steel is considerably higher then in the normalized and annealed steels at the same yield strength level. In regard to dual phase steels previously studied the general conclusion that the threshold level increases with increasing volume fraction of ferrite (from about 35 to 50%) seems to break down in the present case, since present dual-phase steel with approximatively 85% ferrite (Fig.8) shows similar threshold level as the steel with 50% ferrite |7|.

A higher threshold level in duplex microstructure was attributed to the high crack closure level, which in turn was associated with the shear mode crack growth (Mode II) in the near threshold region |7|. The features of the fracture surface observed in this study close to the notch tip (Fig. 5) are

quite similar to the shear mode of fracture observed previously (|7|, Otsuka |22|), but an explanation based on plastic deformation in the ferrite grains being constrained by the martensite encapsulating ferrite thus preventing crack extension by crack tip blunting mechanism (Opening mode I), is not likely to be operative in the present case, since the martensite is not encapsulating ferrite grains (Fig. 8), i.e. martensite connectivity is low and maintained by martensite films at the former ferrite grains (Radmilovic |24|). In the opinion of the present authors an additional experimental evidence is needed before this mechanisms is fully understood.

Data of Fig.4 show that in the stress intensity range used in this work a relation of the form predicted by Paris is obtained. However, in respect to m=2.22 obtained in this work, a value of m=3.32 and m=9.66 reported previously (6) for dual-phase structure consisting of martensite islands (36.4%) in ferrite and ferrite islands in martensite (39.2%) respectively is substantially higher. To clarify this point, a systematic study of effect of volume fraction of martensite and martensite connectivity on the crack growth rate, is apparently needed.

The role of martensite in the crack propagation process may be rationalized as follows. The fatigue crack seems to propagate not only in the ferrite phase (probably by striation mechanism) and along the ferrite martensite interface (by intergranular decohesion) but also through the martensite in spite of there being a continuous ferrite path available for the crack to follow. This seems to be contrary to the behaviour of some ferrite/pearlite steels in which the crack path is preferentially through the free ferrite, while the pearlite colonies act only as mechanical bariers,(Aita et al.|23|).

CONCLUSIONS

1. The fatigue crack initiation threshold $(\Delta K/\sqrt{\rho})_{th}$ decreases from 830 to 720 and 630 MPa with increasing notch tip radius from 0.4 to 0.8 and 1.6 mm respectively.
2. The fatigue crack propagation threshold K_{th} is estimated at 14.7 MPa$\sqrt{m}$.
3. In the near threshold region fatigue crack is propagating not only through the ferrith phase and along the ferrite/martensite interface but also through the martensite.
4. The fatigue crack growth rate as a function of stress intensity range can be described by a relation of the form:

$$da/dN = 2.7\cdot10^{-11}(\Delta K)^{2.22}.$$

REFERENCES

|1| Formable HSLA and Dual-Phase Steels, The Metallurgical Society of AIME, (1979)

|2| Structure and Properties of Dual-Phase Steels, The Metallurgical Society of AIME, (1979)

|3| Fundamentals of Dual-Phase Steels, The Metallurgical Society of AIME, (1981)

|4| Sherman,A.M., and Davies,R.G., Met.Trans. 10A,(1979),929

|5| Kim,Y.H.,and Fine,M.E., Met.Trans. 13A, (1982) 59

|6| Suzuki ,H.,and Mc Evily,A.J., Met.Trans., 10A (1979),475

|7| Minakawa,K.,et al., Met.Trans. 13A, (1982) 439

|8| Radmilović,V.,Drobnjak,Dj. and Rogulić,M., Proceedings of the 4th E.C.F. Conf., Leoben, (1982), 322

|9| Radmilović,V.,Drobnjak,Dj. and Djurić,B., Proceedings of the 4th Riso Symposium, Danmark, (1983), 499

|10| Braglia,B.L., et al, ASTM STP-677, (1979), 290

|11| ASTM Standard E-399, (1974)

|12| ASTM Standard E-647, (1978)

|13| Le Pera,F.S., J. of Metals, 32, (1980), 38

|14| Barsom,J.M. et al, ASTM STP-559, (1974), 183

|15| Rolfe,S.T. and Barsom,J.M., Fracture and Fatigue Control in Structures, Prentice-Hall, Englewood Cliffts, (1977), 208

|16| Smith,R.A. and Miller,K.J., Int.J.Mech.Sci., 20,(1977),201

|17| Fine,M.E., Met.Trans, 11A, (1980), 365

|18| Ritchie,R.O. J.Eng.Mat.and Tech., Ser.H., 1977. **vol.99**, 195

|19| Ritchie,R.O., Met.Sci., 11, (1977), 368

|20| Cooke,R.J. et al.,Eng.Fract. Mech., 7, (1975), **69**

|21| Masounave,J. and Bailon,J.P., Scripta Met., 10, (1976),165

|22| Otsuka,A. et al., Eng.Fracture Mech., 7, (1975), 429

|23| Aita,C.R. and Weertman,J., Met.Trans., 10A, (1979), 535

|24| Radmilović,V., Private communication

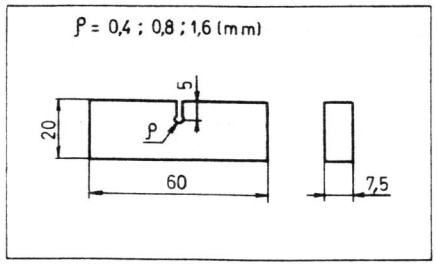

Fig.1 Modified three point bend specimen

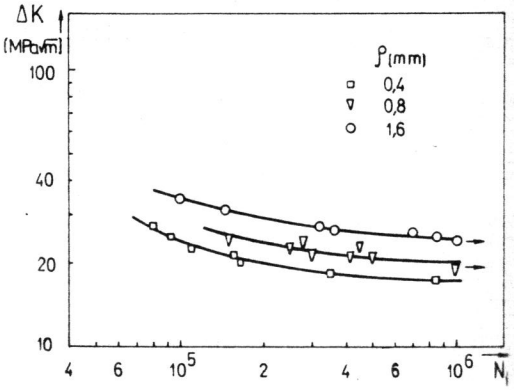

Fig.2 ΔK vs. N_i

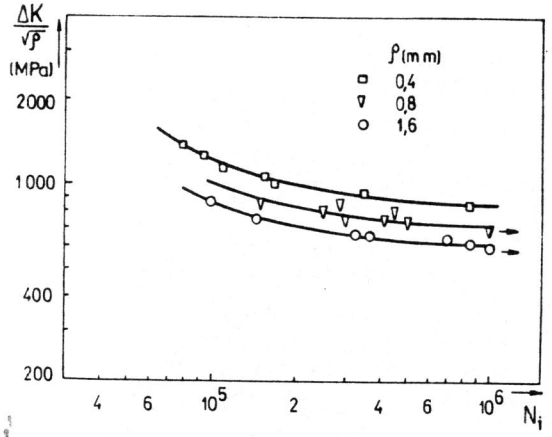

Fig.3 $\Delta K/\sqrt{\rho}$ vs. N_i

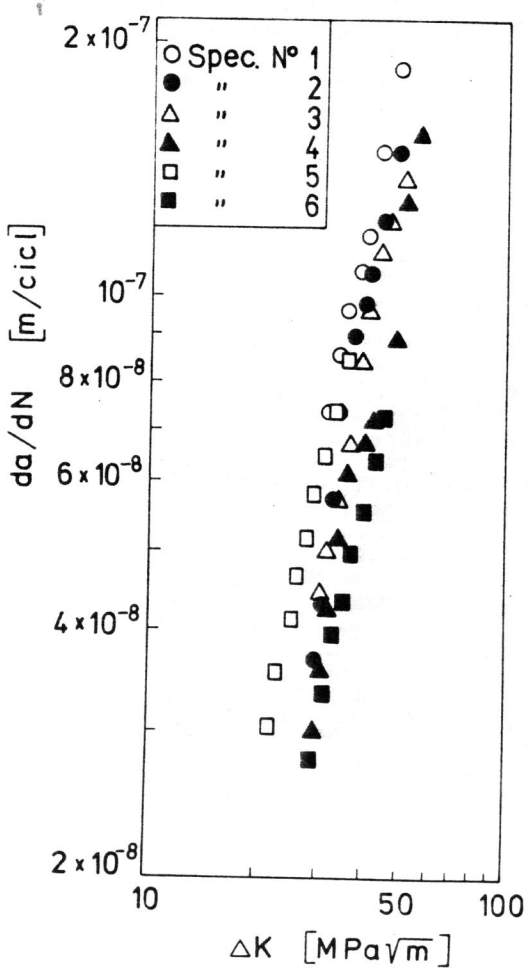

Fig.4 da/dN vs. ΔK

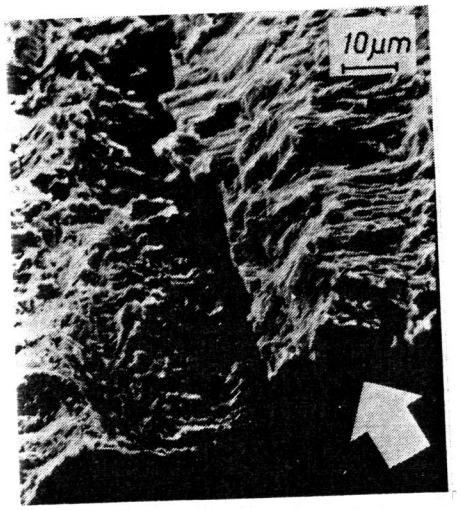

Fig. 5 SEM photograph of fracture surface in near notch tip region, 45 deg tilt, (notch/ /fracture boundary is indicated by arrow).

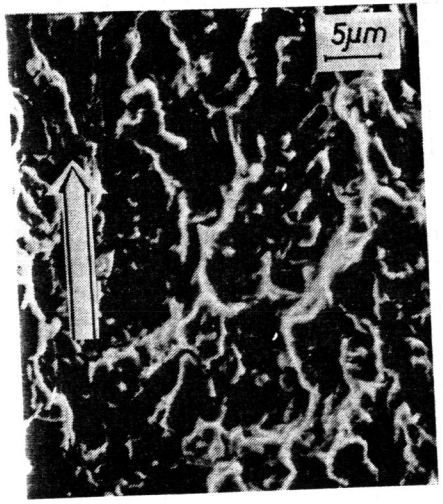

Fig. 6 photograph of fracture surface at $\Delta K=45$ MPa$\sqrt{m}$ (crack growth direction is indicated by arrow).

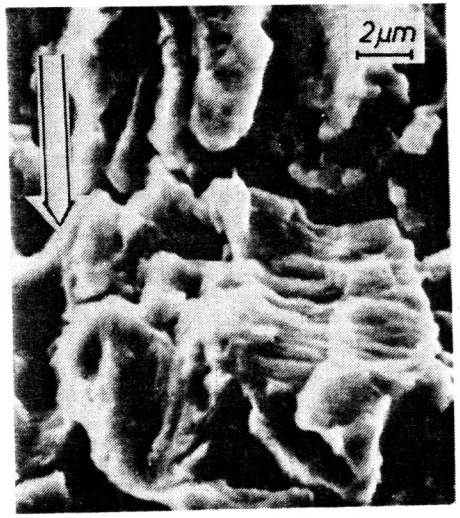

Fig. 7 SEM photograph of fracture surface at $\Delta K=37$ MPa$\sqrt{m}$ (crack growth direction is indicated by arrow).

Fig. 8 Crack path observed by optical microscope near threshold level ($\Delta K\cong 15$ MPa$\sqrt{m}$). In this microphotograph white and black area are martensite and ferrite respectively.